NSTX far infrared tangential interferometer/polarimeter electronics upgrade[a)]

W. C. Tsai,[1] C. W. Domier,[1,b)] K. C. Lee,[1] N. C. Luhmann, Jr.,[1] R. Kaita,[2] and H. K. Park[3]
[1]*Department of Electrical and Computer Engineering, University of California, Davis, California 95616, USA*
[2]*Princeton Plasma Physics Laboratory, Princeton, New Jersey 08543, USA*
[3]*Pohang University of Science and Technology, Pohang, Kyungbuk 790-784, Republic of Korea*

(Presented 17 May 2010; received 17 May 2010; accepted 26 July 2010; published online 25 October 2010)

New electronics for the multichannel far infrared tangential interferometer/polarimeter system employed on the National Spherical Torus Experiment (NSTX) have greatly extended its capability to monitor high frequency density fluctuations. Such measurements are essential in understanding transport physics issues in NSTX as well as for the coming ITER device. The electronics, which were previously limited to ~250 kHz, have been upgraded with a video bandwidth that extends to 4 MHz when operating as an interferometry-only configuration, and to ~500 kHz when operating as a simultaneous interferometer/polarimeter system. Experimental details and test results of the new electronics are presented. © *2010 American Institute of Physics.* [doi:10.1063/1.3485103]

I. INTRODUCTION

The multichannel far infrared tangential interferometer/polarimeter (FIReTIP) system employed on the National Spherical Torus Experiment (NSTX) was designed for electron density and magnetic field measurements as well as real time monitoring of density fluctuations.[1] The system employs a three FIR laser detection technique,[2] permitting simultaneous interferometry and polarimetry measurements with high temporal response. Two 119 μm lasers probe the plasma with right (R-wave) and left (L-wave) circularly polarized waves, while the third laser serves as a local oscillator (LO) source to each receiver. The phase of the R-wave signal provides core-integrated electron density (interferometry) data, while the phase difference between the R- and L-wave components provides magnetic field (polarimetry) data.

Fast time resolution requires a modulation frequency or laser frequency separation significantly higher than the phase change rate. The intrinsic laser linewidth typically limits the maximum separation between any two lasers to ~2 MHz. A critical component in the FIReTIP system is the use of a Stark-tuned laser as the third laser, with which a ~5 MHz Stark shift was demonstrated.[3,4] Despite this advance, however, the FIReTIP video bandwidth and hence temporal resolution were still limited to ~250 kHz. The goal of this work was to extend the temporal resolution to at least several megahertz, approaching the limit set by the Stark-tuned laser.

Section II addresses the bandwidth limitations of the previous electronics system. The new FIReTIP electronics design is described in Sec. III. The temporal resolution capability and noise performance achieved by the new FIReTIP electronics are presented in Sec. IV. Finally, a quantitative comparison of the performance of the FIReTIP electronics with those of other interferometer and polarimeter systems is provided including the significance for other systems.

II. LIMITATIONS OF PREVIOUS ELECTRONICS

The FIReTIP optical system design is detailed in Ref. 4, but is described briefly in the following. Each plasma signal is formed by combining the L- and R-wave beams, propagating the combined beam through the plasma, and then mixing the return beam with the LO beam. With 2 MHz separation between the L- and R-wave lasers, and ~5 MHz Stark shift on the LO laser, this results in each plasma signal containing both 4 MHz (L-wave) and 6 MHz (R-wave) components. A portion of the L- and R-wave beams are separately mixed with the LO beam to form 4 and 6 MHz reference signals, respectively. All plasma and reference signals are extremely low in amplitude (from −110 to −90 dBm, due to high conversion loss mixers), and are amplified by 84 dB before being passed on to the FIReTIP electronics.

A simplified layout of the previous electronics is presented in Fig. 1. The 4 and 6 MHz reference signals are upconverted by 24 MHz and phase-locked to form 28 and 30 MHz reference signals, respectively. The phase-lock loop (PLL) circuits employ a voltage-controlled oscillator (VCO) (MiniCircuits POS-50) with a modulation bandwidth of only 100 kHz that, while sufficient to handle the frequency jitter of the lasers, is not sufficiently fast to be applied to the plasma signals. Each plasma signal is then divided into two parts, separately mixed with the 28 and 30 MHz reference signals, and bandpass filtered at 24 MHz. The bandwidth of these filters is sufficiently narrow to separate the L- and R-wave components, but limits the effective rf bandwidth of each signal from 160 to 500 kHz depending on the center

[a)]Contributed paper, published as part of the Proceedings of the 18th Topical Conference on High-Temperature Plasma Diagnostics, Wildwood, New Jersey, May 2010.
[b)]Author to whom correspondence should be addressed. Electronic mail: email@cwdomier@ucdavis.edu.

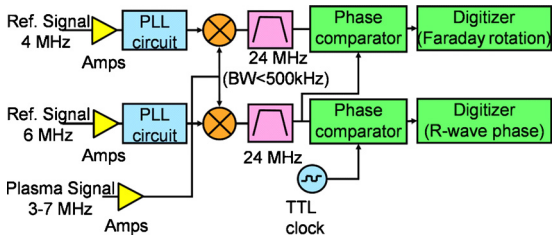

FIG. 1. (Color online) Schematic layout of the old FIReTIP electronics.

frequency and sharpness of the individual filters. The filter outputs are converted into digital signals using zero crossing detectors, and then fed to divide—by 16, 20, and 64 fringe—counter circuits and lowpass filtered at 330, 280, and 85 kHz, respectively. The effective video bandwidth is set by the narrowest bandwidth among the various filters, and thus varies from a low of 150 kHz to a high of 330 kHz for the divide-by-16 circuits.

III. EXPERIMENTAL DESIGN

A. Phase tracking receiver

The phase tracking receiver is basically a PLL consisting of a phase detector or mixer, a lowpass loop filter, and a VCO. The PLL input signal is mixed with a portion of the VCO output signal, generating an error signal related to the phase difference between the two signals. The error signal forces the VCO's frequency to track that of the input signal. The lock-in range is the bandwidth between the margins where the input signal switches from an unlocked to a locked state, and is a measure of the PLL's ability to track rapidly changing signals.

The new electronics employ reduced phase noise VCOs with 6 MHz modulation bandwidths (MiniCircuits ROS-80–7119) for the reference signals and 17 MHz bandwidths (MiniCircuits ROS-70–119) for the plasma signals. Plotted in Fig. 2 are the measured lock-in bandwidths as a function of the input signal level of the new and old PLL circuits. Both lock-in bandwidths are seen to increase from <1 to >11 MHz with increasing signal level, and considerably outperform the old PLL circuitry over a relatively wide signal range. Maintaining lock-in bandwidths >5 MHz, however, requires input signal levels within a relatively narrow range (6 dB) and hence the need for automatic gain control (AGC) circuitry.

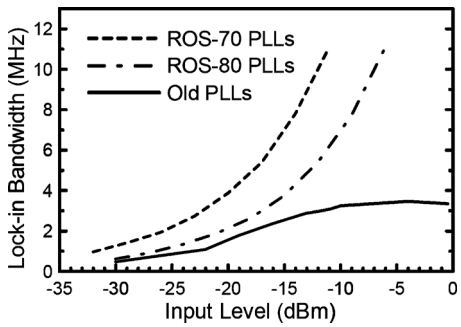

FIG. 2. Measured PLL lock-in range of previous and new PLL circuits as a function of the PLL input signal level.

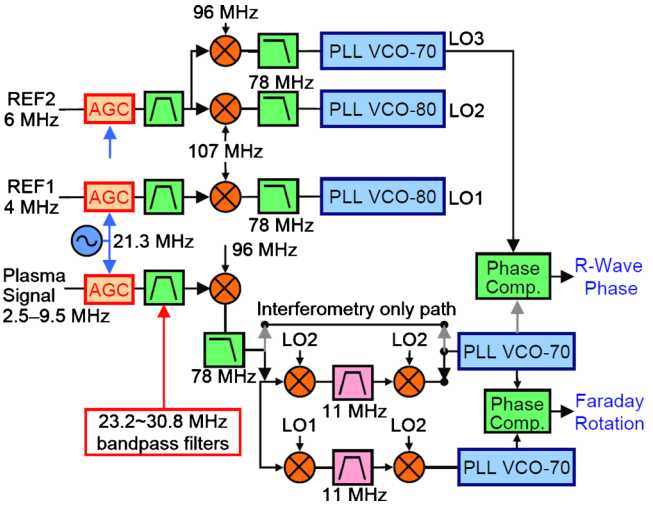

FIG. 3. (Color online) Schematic layout of the wide video bandwidth FIReTIP electronics approach.

B. AGC circuit and upconversion stage

For simultaneous interferometry/polarimetry measurements using the new electronics, each plasma signal component (R- and L-waves) is assumed to have a ± 1 MHz range, yielding a frequency span of 3–7 MHz as in the previous electronics. For interferometry-only measurements, the L-wave laser is turned off and the 6 MHz R-wave signal is assumed to have a ± 3.5 MHz bandwidth spanning 2.5–9.5 MHz. The high modulation bandwidth VCOs require a two-step upconversion process to avoid generating spurious mixer products from the 2.5 to 9.5 MHz signals (now within the modulation bandwidths of the VCOs). This, together with the need to maintain a <6 dB input signal range, means that an AGC circuit is required which simultaneously upconverts the signals to >20 MHz. A second set of mixers then upshifts the AGC outputs to yet higher frequencies corresponding to the ROS-70 and ROS-80 ranges.

The ~ 4 and ~ 6 MHz reference components generate signals LO1 (~ 81.7 MHz), LO2 (~ 79.7 MHz), and LO3 (~ 68.7 MHz) as shown in Fig. 3. The AGC circuits upconvert each 2.5–9.5 MHz plasma signal to 65.2–72.2 MHz. For interferometry-only measurements, these plasma signals are directly compared with that of LO3. For interferometry/polarimetry measurements, these signals are split into two parts, separately downconverted by LO1 and LO2, and bandpass filtered at 11.0 MHz. The sharpness of the KR2163 filters (1 dB passband from 10.69 to 11.29 MHz, 40 dB rejection below 9.79 MHz, and above 12.19 MHz) filters out the unwanted signal components, after which they are mixed back to 65.2–72.2 MHz and compared with that of LO3.

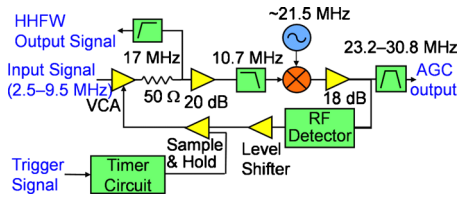

FIG. 4. (Color online) Schematic layout of the AGC circuit.

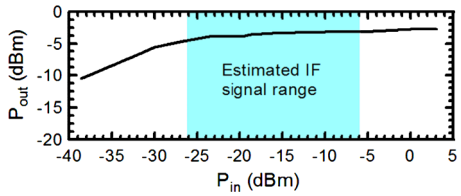

FIG. 5. (Color online) Measured AGC output power as a function of the two-tone (4 and 6 MHz) input power.

FIReTIP preamplifier output signal levels vary from channel to channel and from day to day between −26 and −6 dBm. PLL performance, however, is maximized over a narrow range of input signal levels (see Fig. 2). AGC circuits employ voltage-controlled amplifiers (VCAs) to increase the strength of weak signals and suppress strong signals to maintain a nearly constant output signal level. As the circuit must also upconvert the signal frequencies to >20 MHz, the upconverted signal must then be bandpass filtered using a wide bandwidth filter with high stopband rejection and steep band edges. Here, a KR2473-A filter was selected with a 1 dB bandwidth extending from 23.2 to 30.8 MHz with >60 dB rejection below 19.5 MHz and above 34.5 MHz.

The AGC circuit for the new electronics is shown schematically in Fig. 4. Each input signal is amplified by a low harmonic distortion VCA and then upconverted by 21.3 MHz and sampled by a rf detector to provide feedback to the VCA. The VCA gain setting can be optionally "frozen" through an external trigger signal coupled to a sample-and-hold unit. Also included is a pick-off signal which separates out any ~30 MHz signals arising from density fluctuations induced by high harmonic fast wave heating on NSTX. An output signal variation of only 1.6 dB is achieved over a 20 dB input dynamic range (see Fig. 5), with a measured worst-case two-tone intermodulation level of −42 dBc.

C. Phase comparison electronics

Two phase comparison techniques are employed for phase delay measurements. The first is a digital fringe counter approach, employing divide-by-8 prescalers to transform the 68.7 MHz input and reference signals into 8.6 MHz transistor-transistor logic (TTL) signals. A D-type flip-flop circuit generates a TTL pulse whose duty cycle is proportional to the phase difference between the two signals. The TTL pulse is then lowpass filtered and level-shifted to generate an output voltage that is proportional to that input phase difference, with a 3 dB video bandwidth of 1.0 MHz or ~4 times that of the previous circuit. The output signals are sampled at 2.5 MHz with 14-bit resolution.

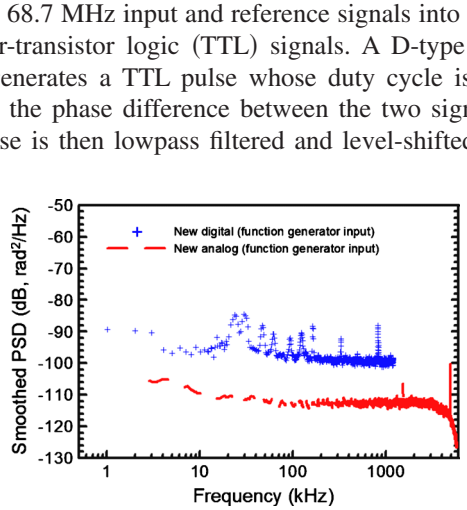

FIG. 6. (Color online) Smoothed phase noise spectra for the new digital (crosses) and analog (dash line) output circuits with the employment of a 5.0 MHz function generator signal to both the reference and plasma signals.

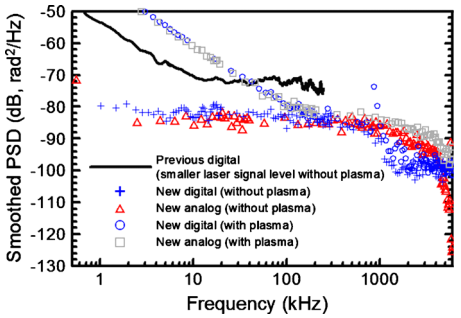

FIG. 7. (Color online) Smoothed phase noise spectra acquired with FIR laser signals for the previous electronics (solid curve), new digital (crosses) and analog (triangles) output circuits under test shots taken without plasma. Plasma results shown in circles for new digital and squares for new analog output circuits.

The second technique is a simpler analog approach employing in-phase (I)-quadrature (Q) demodulators. An I-Q demodulator generates two output signals corresponding to $A^* \sin\theta$ and $A^* \cos\theta$, where A is the amplitude of the plasma signal and θ is the phase difference between the plasma and reference signals. The analog circuit has a video bandwidth of 5.6 MHz and is sampled at 12 MHz.

IV. MEASUREMENT RESULTS

A. PLL temporal resolution

The PLL temporal response has been measured using frequency-modulated input signals, where the modulation frequency emulates the fluctuating plasma signal. A 4 MHz modulation frequency was chosen as that corresponds to half of the KR2473-A filter bandwidth, and therefore provides a hard limit to the achievable temporal resolution in interferometry-only mode. The circuit is observed to maintain locking with modulation levels of up to −10 dBc (FIReTIP phase fluctuation levels are typically <−25 dBc). A temporal resolution of 0.35/(4 MHz)=0.088 μs is thus expected in interferometry-only operation. The 1 MHz-bandwidth filter for R- and L-wave separation in the interferometry/polarimetry mode, on the other hand, limits the temporal resolution to 0.35/(0.5 MHz)=0.7 μs.

B. System phase noise and phase resolution

The electronics have been tested in interferometry-only mode using signal generator inputs, FIR laser inputs without

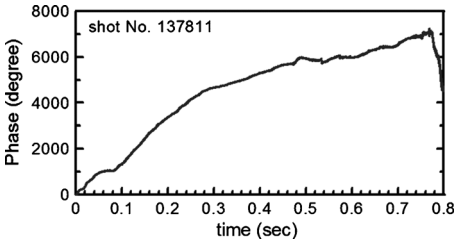

FIG. 8. Phase evolution of interferometry measurements.

TABLE I. Comparison of phase noise performance between the previous, new digital fringe counter, and new I-Q mixer circuits employed in the phase comparator electronics.

Phase comparator electronics	rms phase noise (deg) at offset within 5%				rms phase noise (deg) up to the bandwidth			
	0.01	0.1	1.0	4.0 MHz	0.01	0.1	1.0	4.0 MHz
Previous	0.48	1.2			5.7	7.6		
New analog	0.06	0.23	0.69	0.53	0.39	1.1	3.4	4.8
New digital	0.08	0.28			0.50	1.5	3.2	

TABLE II. Achieved performance of FIR interferometers for major magnetic fusion devices.

Ref.	Wavelength (μm)	Modulation frequency	Video bandwidth	Phase resolution
9	337	10 kHz	4 kHz	0.4°[a]
8	195	100 kHz	1 kHz	18°
7	118.8	1 MHz	2 kHz	12°
5 and 6	118.8	1 MHz	100 kHz	5°
This paper	118.8	5 MHz	100 kHz	5°
			4 MHz	25°

[a]Listed resolution corresponds to digital-to-analog converter resolution only; effective resolution due to finite signal-to-noise ratio is not reported.

plasma, and FIR laser inputs with plasma. Plotted in Fig. 6 is the power spectral density (PSD) for the new circuits in response to a 5.0 MHz signal generator signal applied to both reference and input signals. The electronics are seen to be inherently low noise, corresponding to a 9° root-mean-square (rms) phase resolution for the digital outputs and 2° for the analog outputs.

PSD acquired with FIR laser signals are presented in Fig. 7 together with data collected by the previous FIReTIP electronics under similar conditions. Increased noise arising from low FIR power levels (<20 mW for the LO beam and <50 mW for the rf beam, split among seven mixers) and high mixer conversion losses are seen to significantly degrade the phase resolution achieved with the previous electronics, with a resolution of 21° at its 100 kHz video bandwidth observed but improving to a 5° resolution with a 10 dB increase in FIR power levels. Also observed in Fig. 7 is the rise of low frequency components during plasma operation (shown in circles and rectangular); the complete interferometer trace for this discharge is plotted in Fig. 8. Phase noise calculations for the new and previous electronics (without plasma) are presented in Table I; the relative phase noise is calculated as a function of frequency offset within a 5% bandwidth centered at the offset frequency, and the overall phase noise represents the integrated noise from dc to the offset frequency.

V. DISCUSSION

The upgraded FIReTIP electronics were installed on NSTX in July 2009. The upconverting AGC design and new PLL circuits achieve a temporal resolution of 0.09 μs (4 MHz) for interferometry and 0.7 μs (0.5 MHz) for interferometry/polarimetry operation. The system performance is compared in Table II with other heterodyne interferometer systems[5–9] with analog outputs. Note that systems utilizing digital approach for the raw signals (such as direct digitization or Zebra-stripe interferometers) are excluded from the comparison unless they also include a real-time digital-to-analog converter output. The best published analog phase resolution in a wideband system (bandwidth of at least 100 kHz) is roughly 5° using acousto-optic modulators driven at 1 MHz by a Bragg cell,[5,6] while the current system demonstrates a similar capability but at a 4 MHz bandwidth.

It is worth comparing this approach with others that employ direct digitization of interferometer signals. The digitization approach avoids the need for sophisticated electronics, and can achieve high video bandwidths with respect to their modulation frequencies similar to what has been achieved herein. The downsides are the need for extremely fast digitizers (sampling at least five times the modulation frequency), large data storage, and lengthy computation times required to process the data.

ACKNOWLEDGMENTS

This work is supported by the United States Department of Energy under Contract Nos. DE-FG02-99ER54518 and DE-AC02-09CH11466.

[1] H. Park, C. W. Domier, W. R. Geck, and N. C. Luhmann, Jr., Rev. Sci. Instrum. **70**, 710 (1999).
[2] J. H. Rommers, A. J. Donné, F. A. Karelse, and J. Howard, Rev. Sci. Instrum. **68**, 1217 (1997).
[3] B. H. Deng, H. C. Chen, C. W. Domier, M. Johnson, K. C. Lee, N. C. Luhmann, Jr., B. R. Nathan, and H. Park, Rev. Sci. Instrum. **74**, 1617 (2003).
[4] K. C. Lee, C. W. Domier, M. Johnson, N. C. Luhmann, Jr., and H. Park, IEEE Trans. Plasma Sci. **32**, 1721 (2004).
[5] K. Kawahata, Proceedings of the 28th EPS Conference on Controlled Fusion and Plasma Physics, Funchal, 2001, Vol. 25A, p. 437.
[6] T. Tokuzawa, K. Kawahata, T. Tanaka, Y. Ito, A. Ejiri, and T. Simizu, Rev. Sci. Instrum. **72**, 1103 (2001).
[7] D. K. Mansfield, K. K. Park, L. C. Johnson, H. M. Anderson, R. Chouinard, V. S. Foote, C. H. Ma, and B. J. Clifton, Appl. Opt. **26**, 4469 (1987).
[8] G. Braithwaite, N. Gottardi, G. Magyar, J. O'Rourke, J. Ryan, and D. Véron, Rev. Sci. Instrum. **60**, 2825 (1989).
[9] Y. Zhou, Z. Deng, J. Yi, Y. Li, L. Li, L. Zheng, K. Zhao, Q. Yang, and X. Ding, Plasma Sci. Technol. **11**, 413 (2009).